International Journal of Emerging Trends & Technology in Computer Science (IJETTCS)
Web Site: www.ijettcs.org Email: editor@ijettcs.org
Volume 3, Issue 4, July-August 2014 **ISSN 2278-6856**

AN EFFICIENT LEARNING BASED ALGORITHM FOR LUNG BOUNDARY DETECTION FOR CHEST X-RAY IMAGES

Savitha S. K[1], Aprameya K. S[2], Alwyn R. Pais[3]
[1]Department of Computer Science Engineering,
Bangalore Institute of Technology, Bangalore, Karnataka, INDIA.

[2]Department of Electrical Engineering,
University B.D.T Engineering College,V.T.U
Karnataka, INDIA.

[3]Department of Computer Science Engineering
National Institute of Technology Suratkal.
Karnataka, INDIA

Abstract
We present an algorithm for the automatic delineation of lung boundary fields in chest radiographs. An attempt has been made in this paper to develop a novel mechanism for the detection of lung boundaries. We proposed a new Constrained Active Shape Modeling (CASM) algorithm where ASM algorithm is constrained by the Support Vector Machine (SVM) model parameters during the lung boundary detection in chest x-ray images. Initially the images are preprocessed and subjected to rough segmentation module which generates roughly segmented lung boundaries and then lung boundary specific geometric parameters are computed. In the final stage, later this rough segmentation boundary is used for optimal convergence. Simultaneously we generate a subspace of lung boundary landmark distribution using SVM for all the images in the database. In the next step the detected lung boundary landmark distribution for all the images is subjected to training using ASM algorithm. Finally the rough segmentation lung boundary converges to the optimal lung boundary during CASM application. The proposed method is tested on digital chest image database comprising of various patient populations. The performance evaluation of the proposed method is quantified using degree of overlap between the segmentation result and ground truth result. We also used average contour distance measure to assess the accuracy of lung boundary detection. Both the measures yield promising results in comparison with existing methods.

Keywords – ASM, SVM**,** level sets, edge gradient, X-ray.

1. INTRODUCTION
Detection of lung boundaries in chest radiograph images becomes an important step in computerized analysis of the digital chest radiographs. The chest radiographs play a very prominent role in most of the diagnostic procedures in many general hospitals [1]. In some scenarios the relevant image-based information is extracted directly from the lung boundaries without further analysis. For example, shape irregularity, size measurements and total lung volume [2], [3] provide clues for serious diseases such as cardiomegaly [5], [6], pneumothorax, pneumoconiosis or emphysema [7], [8]. In literature various methods have been applied to segment the lungs from PA chest radiographs. These roughly fall into the following four categories [4]. 1) Rule based methods 2) pixel-based methods 3) hybrid methods that combine rule-based and pixel-based methods 4) Deformable models based methods. The general frame work in the rule based segmentation methods [9], [10] is to detect lung contours for the detection of oriented edges and ridges in images. It is a customized method having a sequence of rules each having specific processing and usually few adjustable parameters. Here segmentation is based around thresholding, edge detection and fuzzy rule-based approach [11]. These methods lead to approximate solutions which are far from the global optimum. Hence, these methods are used only in the initialization stage of the segmentation algorithms. Pixel classification-based methods [12], [13], [14] are more general than rule-based methods. These methods are mainly based on point processing where each pixel of an image classified into either lung field or background using filter bank of Gaussian derivatives at multiple levels and a K-NN classifier. Pixel classification problem calculates a feature vector for each pixel in the input image and outputs the relevant anatomical category to which the pixel belongs to. Deformable models like Active shape models (ASM) [15] and active appearance models (AAM)[16] have been successfully applied to lung field segmentation [17], [18], [19], [20] because of their shape flexibility. In these methods segmentation problem is constrained by the priori knowledge of an object shape, and typically attempt to find the best match between the model and the data in a given new image. Despite these modeling approaches have become popular for biomedical applications, they do have several limitations and shortcomings such as: (i) because of the high contrast and strong rib cage edges many times local minima is trapped, (ii) performance of the segmentation algorithm is entirely depends on the accuracy of initialization to the actual boundary, and (iii)

produces variable solutions since they have many internal parameters. To overcome the above mentioned limitations there are extensions of ASMs for lung field segmentation that are actively being investigated [21], [19], [22], [23]. As an example, in one of the papers in [24], a shape particle filtering approach is used to prevent getting trapped at local minima. Another recent attempt as described in [19] exploits the SIFT descriptors and a shape representation utilizing both population-based and patient-specific shape statistics for matching serial images of the same patient. In literature there are many hybrid methods that aim to produce better results by fusing many other techniques. One example has been discussed in [25] that combine a rule-based and a pixel-based approach. Researchers proposed a graph cuts discrete optimization approach [24] combined with a customized energy function. The graph cuts energy function incorporates atlas shape as prior term that ensures close adherence to normal lung anatomy. In the paper [27] discuss three hybrid approaches by fusing deformation-based and pixel classification methods by choosing the best performing approach using majority voting. In this paper, we propose a robust learning based lung boundary detection algorithm using a shape modeling approach. In order to improve the accuracy of the lung boundary detection we applied a constrained active shape modeling (CASM) mechanism. The ASM algorithm is constrained to work for detection of right lung boundaries by applying SVM model apriority. For the correct identification of the candidate landmark points we decompose the image into multiple resolution levels. We then compute the correct lung boundary landmark distribution subspace at different resolution levels for all the patient populations in the database which is eventually exploited in the ASM algorithm during the training. After the training, the median shape is extracted which is later used as input to ASM. Given a lung image, preprocessing enhances the quality of the image for the detection of the right boundaries. After separating the right and left lung fields we apply a level set evolution in order to roughly segment the fields. We then extract the geometric features for a given chest radiograph for the roughly detected lung boundary fields. Finally the CASM computes the accurate lung boundary points for both the fields. We performed detailed analysis of the proposed method and compared to the state-of-the-art methods using validated Japanese Society of Radiological Technology (JSRT) dataset [28] and India image database.

2. PROPOSED METHOD

The steps incorporated in the proposed method for efficient lung boundary detection in chest x-ray images are explained in the following figure.

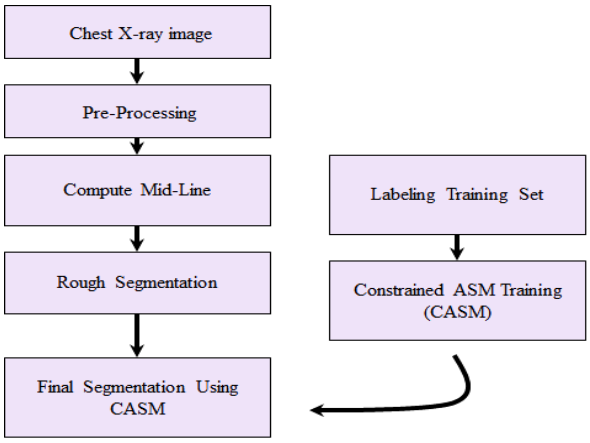

Figure 1: Steps involved in lung boundary detection algorithm.

The rest of the paper is organized as follows. In next section we discuss preprocessing of the images. Sub section 2.2 describes the lung rough boundary segmentation. The proposed CASM algorithm is explained in sub section 2.3 and the final lung boundary segmentation is described in sub section 2.4. Section 3, presents the experimental results and finally summarized remarks are given in section 4.

2.1. Preprocessing

X-Ray lung images are medical images that require a preparation phase in order to improve the quality of the images. In order to speed up the processing, the images are down sampled from 2048x2048 to 256x256. In the next step smooth image is derived by applying 2-D Gaussian operator and simultaneously preserving the edge features and remove the noise. Our method exploits 7x7 kernels as a convolution filter. Followed by image smoothing the contrast level of the lung image is stretched within [μ-σ/2, μ+σ/2]. μ and σ are the mean and standard deviation of the intensity distribution function to enhance the local features. The preprocessed Lung image is shown in Figure 2.

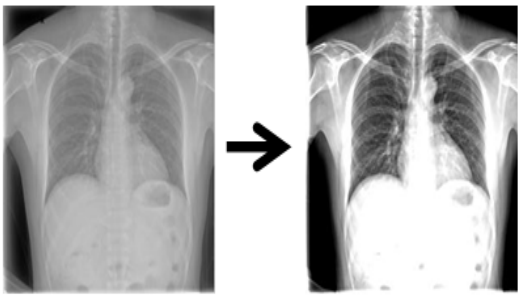

Figure 2: Lung image after preprocessing. The first image to left is before preprocessing and the image to right is after preprocessing.

Since the left and right lung fields need to be processed separately the middle sectional line between the two fields is extracted by projecting the pixel intensity levels, sum them for each column index and then pick the positions of the maximum two peaks x1 & x2 as shown in Figure 3.

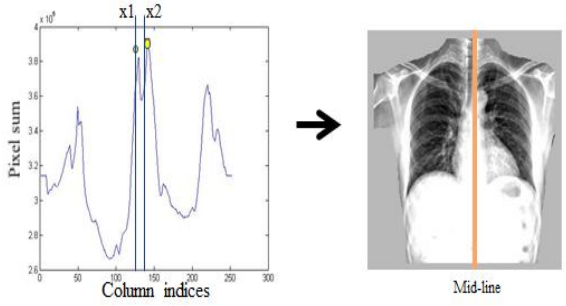

Figure 3: The first image to left is intensity profile and the image to right is mid line detected lung image.

2.2. Lung Rough Segmentation

The initial binary edge image for each lung field is computed by using edge gradient method which acts as initial contour for the lung field and subjected to evolution using the level set approach. The lung contour is converged to lung field boundary after almost 60 iterations. The roughly segmented lung fields are shown in the Figure 4.

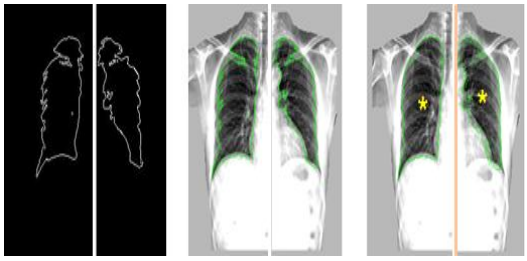

Figure 4: The first image to the left is initial edge detected binary image, the middle image is the edge information projected on to the lung boundary and the image to the right is converged roughly segmented lung fields with the centroids evaluated.

For given x-ray images three statistical parameters are evaluated for each of the lung fields extracted from the level set evolution in the rough segmentation such as lung contour orientation, scale for right and left lungs and position of centroids. We compute lung orientation of each lung boundary pixel on the contour of an roughly segmented image *I(x,y)* using the following equation.

$$\Theta = \frac{1}{2}\arctan\left(\frac{2\mu'_{11}}{\mu'_{20}-\mu'_{02}}\right) \qquad (1)$$

Where:

$$m'_{20} = m_{20}/m_{00} = M_{20}/M_{00} - \bar{x}^2$$

$$m'_{02} = m_{02}/m_{00} = M_{02}/M_{00} - \bar{y}^2$$

$$m'_{11} = m_{11}/m_{00} = M_{11}/M_{00} - \bar{x}\bar{y}$$

$$m'_{11} = m_{11}/m_{00} = M_{11}/M_{00} - \bar{x}\bar{y}$$

$$M_{ij} = \sum_x \sum_y x^i y^i I(x,y)$$

$$\bar{x} = \frac{M_{10}}{M_{00}}, \quad \bar{y} = \frac{M_{01}}{M_{00}}$$

M_{ij} is moment of grayscale image with pixel intensities I(x, y). m_{pq} is an central moment of an image I(x,y) which is given by

$$m_{pq} = \sum_x \sum_y (x-\bar{x})^p (y-\bar{y})^q f(x,y)$$

The scaling factor between the roughly segmented lung boundary and the median lung boundary shapes for both the right and left lung fields is calculated using the following equation.

$$scalingfactor = \frac{A_l}{A_m} \qquad (2)$$

Where A_l is the area of level set result.

A_m is the area of median shape.

The third geometrical attribute that characterizes the roughly segmented lung boundaries is centroid. The centroids for both the right and left lung fields are computed using the equation described below.

$$\{x, y\} = \{M_{10}/M_{00}, M_{01}/M_{00}\} \qquad (3)$$

Where: M_{00} is sum of gray levels of an image.

2.3. Constrained ASM Algorithm

Normally shape of an object is considered as a statistical model that is characterized by set of points that iteratively deforms to fit the shape of the object in a new image. Objective in a classical ASM algorithm is to generate a shape in a given image using geometric features and static profile models of the object such that the shape is representative of the object. Use of the static profile models in ASM during boundary detection quite often leads to the detection of more false positives. In order to get rid of this problem we explored the dynamic 2D profile based ASM method for shape modeling such that the algorithm can detect the lung boundaries of the patient population of any age group. The proposed algorithm is constrained by the dynamic 2D profiles computed from support vector machine for the accurate detection of lung boundary points. In the constrained ASM (CASM) algorithm our objective is to reduce the detection of false positives by building the more robust subspace of lung boundary landmark distribution for each lung field using linearly separable mathematical model called Support vector machine (SVM) [29]. We then apply ASM algorithm on this subspace of lung boundary landmark distribution for all the chest X-ray images in the database and the median shape is finally extracted during the training phase. Here the least median square fit technique is used such that the training data set ensembles the population from large to small aligned and misaligned shapes while doing the lung boundary extraction calculations. We use an interactive segmentation tool for labeling the lungs of the chest radiographs as a first check and subsequently reviewed by expert radiologists. These labeling serves two purposes: one is used as initial reference in the training phase and other for ground truth evaluation. The accurate

computation of the median shape lung boundary comprises of the following steps: The fact that there is shift of the lung boundary edge point at multiple image resolutions becomes the primary reason for exploring the multi resolution 2-dimensional profile analysis. Therefore each image from the image database is decomposed to L/4 levels if L is the length of the first level. As a first step, for each lung boundary pixel from labeled lung boundary image we determine local 2-dimensional profile in order to distinguish the frequency changes in an image. In order to derive the 2-dimensional profile the pixel distribution in each image in training database is globally first equalized by balancing the distribution of the image pixels across the image and subsequently textural frequency image matrix is evaluated by applying a weighted Laplacian filter. The textural frequency image matrix is representative of the 2- dimensional profile. These 2-dimensional profiles (g) are evaluated for multiple resolutions. The weight of the Laplacian filter is adaptable for each patient population and it is estimated based on the results obtained from the images for different patient population. The weights of the Laplacian filter for different patient population are described in below table:

Large Adult	2.11
Medium Adult	1.75
Small Adult	1.45
Pediatric	1.05

At each resolution level we further enhance the normalized image matrix by fitting the candidate edge points along the boundary using the following equation.

$$r_2(g) = (t - I)(g - \hat{g})^T U_g^{-1} (g - \hat{g}). \quad (4)$$

Where **I** describe the gray value at potential point that has the value 0 (for the point not on the boundary) or 1 (for the point on the boundary). **I** is obtained by enhancing the edge by applying the Laplacian filter. g describes the candidate profile vector for each edge point around the labeled landmarks, ĝ characterizes the average profile vector for each candidate edge point around the landmarks and U_g is the covariance matrix of all the vectors across multiple image resolutions. **t** is a constant which is adaptable based on each patient population and it is characterized by performing experiments on images of different patient categories as described in the following table.

Large Adult	2.21
Medium Adult	1.85
Small Adult	1.53
Pediatric	1.17

Secondly in proposed method, we then exploited the linear SVM for the classification of false positives and true positives. The false positive landmark samples randomly select a window which has same size and different focal point with true positive landmarks from the lung boundary point distribution space such that weighted Mahalanobis distance is the smallest. Searching for a candidate lung boundary point is done around the current boundary point to compute the new lung boundary landmark for every image in the database. Candidate landmarks detected on an example of digital lung image from the training image database is shown in Figure 6. X:Input lung boundary shape. For each point (x_i, y_i) of X For each window having focus point (x',y') which belongs to the window with focus point (x_i, y_i). Then apply SVM in the window (x',y'). If the return value is +1 then the point (x',y') lies on the boundary, otherwise returns -1. By electing a point (x',y') for which the value of function r2(g) is the smallest. Then this point becomes the new lung boundary landmark.

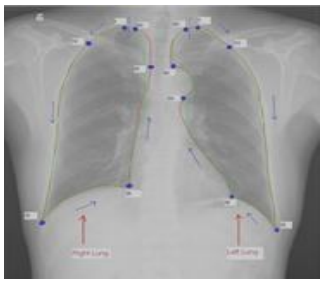

Figure 5: Image describes identified lung landmark distribution for the candidate lung boundary after applying SVM.

Finally the median shape is extracted from the population of misaligned and aligned shapes of the lung boundaries in the image database. The median shape obtained after CASM training using JSRT and Indian image database shown in Figure 6.

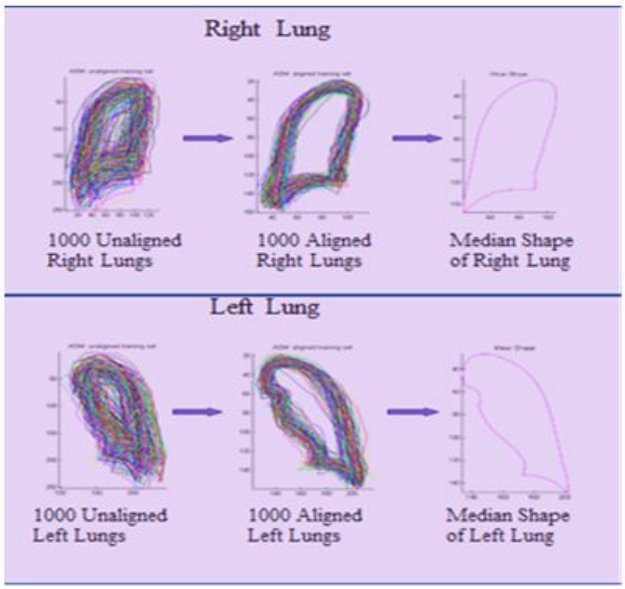

Figure 6: Median lung boundary shape of left and right lungs. This shape is converged to optimal boundary after training.

2.4 Final Segmentation of Lung Fields

The geometrical features such as lung orientation, scaling factor and centroids of the lung fields and the median shape of the lung boundary curve after CASM training

are used as initial input parameters for CASM algorithm. CASM algorithm then computes the optimal lung boundary for each lung field in the chest radiographs. The final segmentation results of the chest radiographs from the image database are shown in Figure 8.

3. EXPERIMENTAL RESULTS

3.1 Chest X-Ray Image Database Formation

We assessed the proposed lung segmentation algorithm using different categories of the chest x-ray (CXR) image datasets. One of the commonly used and publicly available databases for evaluating lung segmentation is the JSRT dataset [28]. We considered both the normal and abnormal lung shapes from the JSRT image database. This image database comprises of 247 chest x-rays, out of which 154 are normal lung, and 93 abnormal lung images. In addition to this image database we have collected around 857 digital chest x-ray images of patients of different age groups from the reputed medical research centers in India. In total, we created a common chest x-ray image database by combining JSRT and Indian image dataset. Evaluation of the proposed segmentation algorithm is done on all kinds of the normal and abnormal lung shapes of different patient populations from this common image database. All the x-ray images in the database have image resolution of 2048×2048 pixels. We generated gold standard segmentations by using an interactive segmentation tool for a quick first segmentation pass through the dataset. The tool automatically detects edges, allowing us to obtain an outline of the lung boundaries with just a few mouse clicks. But, these contours are not accurate and jagged in the first pass, so in a second pass the segmentation results are reviewed by many expert radiologists from reputed medical research centers.

3.2 Evaluation Measures

We evaluated the performance of the proposed algorithm with the existing algorithms using the following measures.

A. The Jaccard similarity coefficient (λ):

This measures the degree of overlap between the ground truth boundary and the estimated segmentation boundary over all pixels in a given chest x-ray image. λ is described in the following equation.

$$Degree\ of\ Overlap = \frac{GroundTRUTHmask \cap Segmentation\ mask}{GroundTRUTHmask \cup Segmentation\ mask} \quad (5)$$

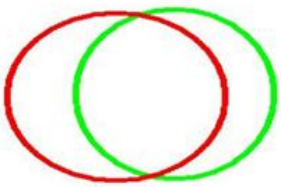

Figure 7: Pictorial description on how the overlap measure is computed.

Region with green curve is segmentation result as shown in Figure 7. This is compared with ground truth which is colored in red. Larger the overlap with ground truth is, better the segmentation performance. Degree of overlap is computed for all the segmented lung images. Average degree of overlap (λ) is evaluated as a measure of the performance of the algorithm.

B. Average contour distance (ACD):

This measure computes the average distance between the estimated segmentation boundary S and the ground truth boundary GT. Let a_i and bj be the points on the boundary S and GT, respectively. The minimum distance of point a_i on S to the GT boundary is evaluated as described below.

$$d(a_i, GT) = \min_j \left\| b_j - a_i \right\| \quad (6)$$

Then the minimum distance for each point on the boundary S to the contour GT is computed. These distances are averaged over all points of boundary S. In order to make the similarity measure symmetric, the computation is repeated from contour GT to contour S using the below equation..

$$ACD(S, GT) = \frac{1}{2}\left[\frac{\sum_i d(a_i, GT)}{|\{a_i\}|} + \frac{\sum_j d(b_j, S)}{|\{b_j\}|}\right] \quad (7)$$

3.3 Computational Speed of Lung Segmentation Algorithm

Implementation of the proposed algorithm is done using the MATLAB programming. We reported the execution times of our lung segmentation algorithm on a desktop personal computer with a 3.12 GHz Intel Xeon CPU and 6 GB of memory in Table 1.

Table 1: Execution times in seconds of the proposed segmentation algorithm on JSRT and India image database at different resolutions.

Resolution	Execution time	λ of JSRT dataset
256x256	15-20s	0.9786±0.021
512x512	50-75s	0.9712±0.019
1024x1024	155-170s	0.9650±0.024

3.4 Algorithm Comparison

In literature many have presented good segmentation results on chest radiographs. Ginneken et al. [25] discussed several pixel classifier algorithm scores to compare their rule-based scheme. In the subsequent papers [31], results on some early segmentation algorithms are listed. In year 2006, the same research group [27] delineated lung, heart, and clavicle boundaries of the JSRT set [28] under the supervision of a radiologist. We performed the following to assess the accuracy of our proposed method. As discussed in section 2.3, lung boundary contours were drawn by radiologists independently, and it is dataset together with the results reported in the literature [30]. The accuracy of our proposed system is λ = 0.9786 ± 0.021. Lung boundary segmentation results on different image datasets with the

above accuracy level are shown in Figures 8 and 9 respectively.

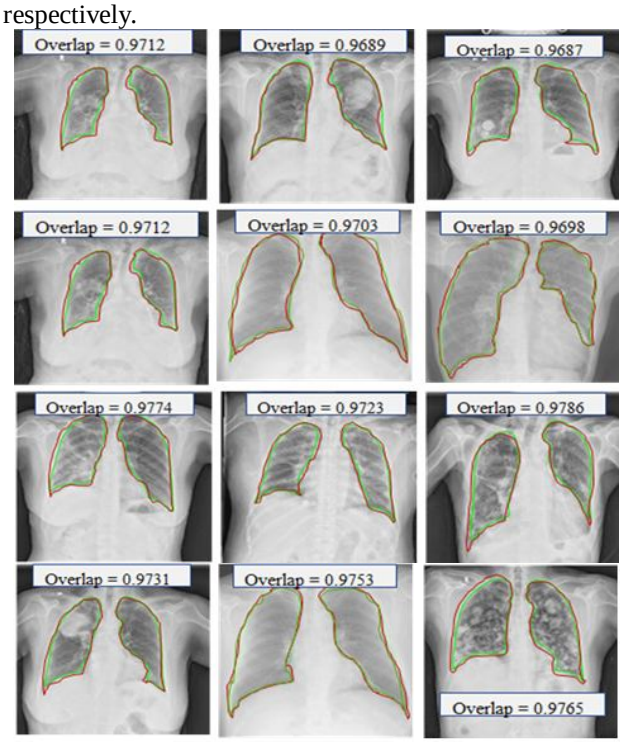

Figure 8: Segmentation results on JSRT and India image datasets. Red and Green indicate the gold standard and automatic segmentation results, respectively.

Table 2: Degree of Overlap (λ) measures of the algorithms reported in the existing methods in comparison with proposed method.

Methods	Overlap measure (λ)
Proposed Method	0.978±0.021
Hybrid voting [3]	0.949±0.020
PC postprocessed [3]	0.945±0.022
Human Observer [3]	0.946±0.018
Fusing Intensity and Shape priors [29]	0.94±0.053
Hybrid ASM-PC [3]	0.934±0.037
Hybrid AAM-PC [3]	0.933±0.026
MISCP [31]	0.930±0.045
ASMOF [24]	0.927±0.032
Fuzzy-Curve [11]	0.927±0.033
ASM-SIFT [26]	0.920±0.031
ShaRC [30]	0.907±0.033
ASM-tuned [3]	0.903±0.057
ASM [26]	0.870±0.074
AAM [3]	0.847±0.095
Mean Shape [3]	0.713±0.075

Table 3: Average Contour Distances (ACD) of the existing methods in comparison with the proposed method.

Methods	ACD
Proposed method	1.210±0.156
Fuzzy-Curve [11]	1.730±0.870
Fusing Intensity and Shape proirs [29]	2.460±2.060

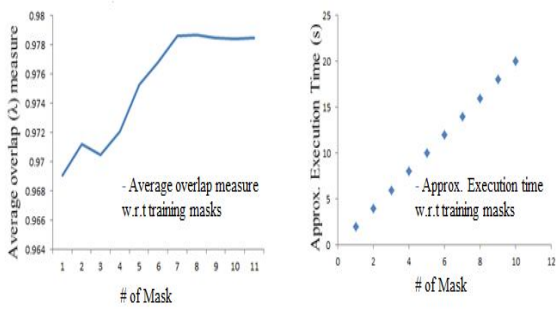

Figure 9: (a) Segmentation Accuracy Evaluation (b) Execution time of the proposed algorithm with respect to training masks (Execution time is measured at resolution of 256x256).

4. CONCLUSION

In this paper, we proposed a novel constrained ASM algorithm where ASM algorithm is constrained by the SVM model parameters during the lung boundary detection in chest x-ray images. Initially we preprocessed and roughly segmented the image. In order to obtain optimal lung boundary we applied CASM learning algorithm using JSRT and Indian image database. In CASM technique we computed 2 dimensional profiles at different resolution levels and accurately classify the lung boundary land marks using SVM model. Finally the detected lung boundary landmark distribution is subjected to training using ASM algorithm to obtain optimal lung boundary convergence. At the end the rough segmentation lung boundary converges to the optimal lung boundary using CASM output and lung boundary geometric parameters. The proposed method outperforms on the chest x-ray images of different categories compared to existing lung boundary detection methods. The performance evaluation of the proposed method is quantified using degree of overlap between the segmentation result and ground truth result. We also used average contour distance measure to assess the accuracy of lung boundary detection. Both the measures yield promising results. Experimental results showed that the proposed method is faster and provide better results when compared to the existing methods.

References

[1] R. E. Bunge and C. L. Herman" Use of diagnostic imaging procedures": a nationwide hospital study. Radiology, 163:569–573, 1987.

[2] J. Paul, M. Levine, R. Fraser, and C. Laszlo, "The measurement of total lung capacity based on a computer analysis of anterior and lateral radiographic chest images," IEEE Trans. Biomed. Eng., vol. 21, pp.444–451, 1974.

[3] F. Carrascal, J. Carreira, M. Souto, P. Tahoces, L. Gomez, and J. Vidal,"Automatic calculation of total lung capacity from automatically traced lung boundaries in postero-anterior and lateral digital chest radiographs," Med Phys., vol. 25, no. 7, pp. 1118–1131, 1998.

[4] Bram van Ginneken and Max A.Viergever, "Computer-aided diagnosis in chest radiography-a survey," IEEE Transactions on Medical Imaging, vol. 20, no. 12, pp. 1228–1241, 2001.
[5] H. Becker, W. Nettleton, P. Meyers, J. Sweeney, and C. Nice, "Digital computer determination of a medical diagnostic index directly from chest x-ray images," IEEE Trans. Biomed. Eng., vol. 11, pp. 67–72, 1964.
[6] G. Coppini, M. Miniati, S. Monti, M. Paterni, R. Favilla, and E.M Ferdeghini, "A computer-aided diagnosis approach for emphysema recognition in chest radiography," Medical Engineering and Physics, vol. 35, no. 1, pp. 63 – 73, 2013.
[7] G.L. Snider, J.L. Klinerman, W.M. Thurlbeck, and Z.H. Bengali, "The definition of emphysema," Report of a national hearth, lung, and blood institute, division of lung disease workshop, vol. 132, pp. 182–185, 1985.
[8] M. Miniati, G. Coppini, S. Monti, M. Bottai, M. Paterni, and E.M. Ferdeghini, "Computer-aided recognition of emphysema on digital chest radiography," European Journal of Radiology, 2010.
[9] Li, Y. Zheng, M. Kallergi, and R.A. Clark, "Improved method for automatic identification of lung regions on chest radiographs," Academic Radiology, vol. 8, no. 7, pp. 629–638, 2001.
[10] P. Annangi, S. Thiruvenkadam, A. Raja, H. Xu, X. Sun, and L. Mao, "A region based active contour method for x-ray lung segmentation using prior shape and low level features," Int. Symp. Biomedical Imaging: From Nano to Macro, pp. 892–895, 2010.
[11] Park, W., Hoffman, E. A., & Sonka,"Segmentation of Intra thoracic Airway Trees:A Fuzzy Logic Approach,"IEEE Transactions On Medical Imaging , 1998.
[12] P. Annangi, S. Thiruvenkadam, A. Raja, H. Xu, X. Sun, and L. Mao, "A region based active contour method for x-ray lung segmentation using prior shape and low level features," Int. Symp. Biomedical Imaging :From Nano to Macro, pp. 892–895, 2010.
[13] Z. Yue, A. Goshtasby, and L. Ackerman, "Automatic detection of rib borders in chest radiographs," IEEE Trans. Medical Imaging, vol. 14, pp. 525–536, 1995.
[14] M. Loog and B. Ginneken, "Segmentation of the posterior ribs in chest radiographs using iterated contextual pixel classification.," IEEE Trans. M Medical Imaging, vol. 25, pp. 602–611, 2006.
[15] T. F. Cootes, C. J. Taylor, D. H. Cooper, and J. Graham, "Active shape models - their training and application," Comput. Vis. Image Understand., vol. 61, no. 1, pp. 38–59, 1995.
[16] T.F. Cootes, G.J. Edwards, and C.J. Taylor, "Active appearance models," IEEE Trans. Pattern Anal. Mach. Intell., vol. 23, no. 6, pp. 681–685, 2001
[17] B. Ginneken, A.F. Frangi, J.J. Staal, B.M. Romeny, and M.A. Viergever, "Active shape model segmentation with optimal features," IEEE Trans. Medical Imaging, vol. 21, no. 8, pp. 924–933, 2002.
[18] B. Ginneken, S. Katsuragawa, B.M. Romeny, K. Doi, and M.A.Viergever, "Automatic detection of abnormalities in chest radiographs using local texture analysis," IEEE Trans. Medical Imaging, vol. 21, no.2, pp. 139–149, 2002.
[19] Y. Shi, F. Qi, Z. Xue, L. Chen, K. Ito, H. Matsuo, and D. Shen, "Segmenting lung fields in serial chest radiographs using both populationbased and patient-specific shape statistics," IEEE Trans. Medical Imaging, vol. 27, no. 4, 2008.
[20] T. Xu, M. Mandal, R. Long, I. Cheng, and A. Basu, "An edge-region force guided active shape approach for automatic lung field detection in chest radiographs," Computerized Medical Imaging and Graphics, vol. 36, no. 6, pp. 452 – 463, 2012.
[21] D. Seghers, D. Loeckx, F. Maes, D. Vandermeulen, and P. Suetens, "Minimal shape and intensity cost path segmentation," IEEE Trans. Medical Imaging, vol. 26, no. 8, pp. 1115–1129, 2007.
[22] A. Dawoud, "Lung segmentation in chest radiographs by fusing shape information in iterative thresholding," IET Computer Vision, vol. 5, no.3, pp. 185–190, 2011.
[23] T. Yu, J. Luo, and N. Ahuja, "Shape regularized active contour using iterative global search and local optimization," IEEE Computer Society Conference on Computer Vision and Pattern Recognition, vol. 2, pp. 655–662, 2005.
[24] M. Bruijne and M. Nielsen, "Shape particle filtering for image segmentation," Medical Image Computing and Computer-Assisted Intervention, vol. 3216, pp. 168–175, 2004.
[25] B. Ginneken and B. Romeny, "Automatic segmentation of lung fields in chest radiographs," Med Phys., vol. 27, no. 10, pp. 2445–2455, 2000.
[26] S. Candemir, S. Jaeger, K. Palaniappan, S. Antani, and G. Thoma,"Graph-cut based automatic lung boundary detection in chest radiographs,"IEEE Healthcare Technology Conference: Translational Engineeringin Health & Medicine, pp. 31–34, 2012.
[27] B.Ginneken,M. Stegmann, and M .Loog,"segmentation of anatomical structures in chest radiographs using supervised methods :a comparative study on a public data base"Medical Image Analysis, vol. 10, no. 1, pp. 19-40,2006
[28] Japaneese Society of Radiological Technology, http://www.jsrt.or.jp/
[29] C. Cortes and V. Vanpik. "Support Vector Networks". Machine Learning, pp. 273-297, 1995.
[30] Sema Candemir ,Stefan J "Lung Segmentation in Chest Radiographs Using Anatomical Atlases with Non-rigid Registration" , IEEE Transactions on

Medical Imaging,vol. 10,no. 10, 2013.
[31] B.Ginneken,B.Romeny,andM.Vierever,"Computer_aided diagnosis in chest radiography:A Survey." IEEE Trans.MedicalImaging,vol.20,no.12,pp.1228 1241,2001.

AUTHOR

Dr K S Aprameya received BE in electrical and electronics engineering from University of Mysore in 1989, M.Tech in digital electronics and communication systems from University of Mysore in 1993 and Ph.D in Electrical Engineering from Indian Institute of Technology, Roorkee in 2009. His research area is in ultrasonic instrumentation systems and signal processing. He is a member of ISTE, member of the Institution of Engineers (India) MIE and member of Ultrasonic Society of India of National Physical Laboratory (CSIR) . His areas of interest are in signal and image processing.

Alwyn Roshan Pais received the B.Tech degree in Computer Engineering from Mangalore University, Karnataka and M. Tech Degree in Computer Science and Engineering from IIT Bombay. He has submitted his Ph.D. thesis in the area of Computer Vision. He is an Assistant Professor in the Department of Computer Science and Engineering at NITK-Surathkal , Mangalore, India. His research interests include Information Security, Network Security, Cryptography and Computer Vision.

Savitha S.K received the B.E degree in Computer Science and Engineering from Bangalore University, Karnataka and M. Tech Degree in Computer Science and Engineering from Kuvempu University Karnataka. She is pursuing Ph.D. in V.T.U, Karnataka in the area of Medical image processing. She is an Assistant Professor in the Department of Computer Science and Engineering at B.I.T, Bangalore, Karnataka, India.